

Oct 26th, 12:00 AM

Cold-formed Steel Angles under Axial Compression

Y. Shifferaw

Maximiliano Malite

Benjamin W. Schafer

Gustavo M. B. Chodraui

Follow this and additional works at: <https://scholarsmine.mst.edu/isccss>



Part of the [Structural Engineering Commons](#)

Recommended Citation

Shifferaw, Y.; Malite, Maximiliano; Schafer, Benjamin W.; and Chodraui, Gustavo M. B., "Cold-formed Steel Angles under Axial Compression" (2006). *International Specialty Conference on Cold-Formed Steel Structures*. 1.

<https://scholarsmine.mst.edu/isccss/18iccfss/18iccfss-session4/1>

This Article - Conference proceedings is brought to you for free and open access by Scholars' Mine. It has been accepted for inclusion in International Specialty Conference on Cold-Formed Steel Structures by an authorized administrator of Scholars' Mine. This work is protected by U. S. Copyright Law. Unauthorized use including reproduction for redistribution requires the permission of the copyright holder. For more information, please contact scholarsmine@mst.edu.

Eighteenth International Specialty Conference on Cold-Formed Steel Structures
Orlando, Florida, USA, October 27 & 28, 2006

COLD-FORMED STEEL ANGLES UNDER AXIAL COMPRESSION

G.M.B. Chodraui¹, Y. Shifferaw², M. Malite¹, B. W. Schafer²

(1) Department of Structural Engineering
School of Engineering of Sao Carlos – University of Sao Paulo
Av. Trabalhador Sao-Carlense, 400 - CEP 13566-590 - Sao Carlos, SP Brazil
(email: mamalite@sc.usp.br)

(2) Department of Civil Engineering
Whiting School of Engineering – Johns Hopkins University
3400 N. Charles St., Baltimore MD, 21218 – U.S.A
(email: schafer@jhu.edu)

ABSTRACT

The objective of this paper is to examine the stability and strength of concentrically loaded cold-formed steel angles as determined by (i) numerical methods, (ii) experiment, and (iii) effective width and Direct Strength based design methods. In addition, the imperfection sensitivity and interaction amongst the stability modes in cold-formed steel angle columns is studied. The elastic stability of cold-formed steel angle columns is examined primarily with the finite strip method to show that the coincident local-plate/global-torsional mode has some important behavior when multiple buckling half-wavelengths are considered along the length. A series of tests on single and double angles, recently conducted at Sao Paulo, are detailed and the results used to examine existing design methods. The results indicate that the design practice of ignoring local/torsional buckling as a global mode and only considering it as a local mode may not be conservative in some circumstances. This conclusion is further supported and discussed in an extended set of nonlinear finite element analysis.

1. Introduction

A concentrically loaded cold-formed steel angle column is seemingly the most simple of cold-formed steel shapes. However, slender angles suffer from at least two types of instability (i) local-plate/global-torsional instability and (ii) flexural buckling about the primary axes. Though conservative design methods exist, the exact means with which local/torsional instability should be treated in design remains an open question. As do related questions on sensitivity to imperfections (or eccentricities), the extent to which the buckling modes interact with one another, interaction with yielding, and the importance of shifts in the centroid of locally unstable angles.

This paper begins with an examination of the elastic stability of cold-formed steel angle columns with particular attention paid to the coincident local-plate/global-torsional mode. Subsequently, recent testing performed at Sao Paulo on angle columns is detailed (Chodraui & Malite 2005), along with experiments previously conducted by others. Next, the test results are compared with simplified effective width and Direct Strength design methods. Finally, nonlinear finite element (FE) analysis of the Sao Paulo tests along with extended FE studies are performed to further examine the impact of imperfections and the interaction of stability modes on the ultimate strength of angles.

2. Elastic Stability

The elastic stability of a slender angle in compression is typically concerned with two modes: local-plate/global-torsional and flexural. For example, the stability of a 60 mm x 60 mm x 2.38 mm angle in pure compression is assessed in Figure 1 through the finite strip method (FSM) in CUFSM (Schafer 2006). The analysis provides the buckling load P_{cr} as a function of the buckling half-wavelength. Two modes are identified in Figure 1a, solid lines indicate the first mode and dashed lines the second mode, at a given half-wavelength. The first mode, identified as local/torsional in Figure 1a, is unusual in comparison with finite strip analysis of lipped channels and other conventional cold-formed steel members because (i) no minimum exists as a function of half-wavelength, (ii) local and torsional buckling are coincident, and (iii) distortional buckling is not identified.

Local-plate and global-torsional buckling are mathematically coincident for equal leg angles, of constant thickness, concentrically loaded, e.g., Rasmussen (2003) shows this fact explicitly. The coincidence of a local-plate mode with a global-member mode causes some confusion and question in cold-formed steel member design where the inclusion of local-global interaction is generally considered critical to accurate and conservative member design.

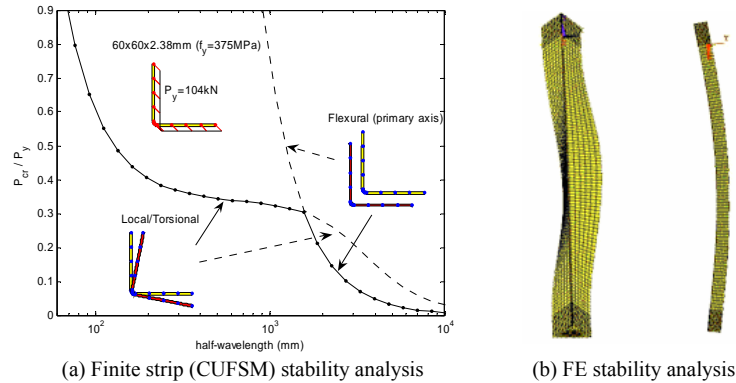


Figure 1 Stability analysis of a cold-formed steel angle column

In considering how the elastic stability modes of an angle may, or may not, interact it is useful to understand more deeply how local/torsional or flexural buckling may occur when more than one half-wavelength occurs in a given member length, L . For finite strip analysis, the actual buckling mode shape, ϕ , is:

$$\phi = (2D \text{ mode shape}) \sin(m\pi z/L) \quad (1)$$

where the 2D mode shape is the deformed shape identified in Figure 1a, m = number of half-waves in length L ($m=1$ in Figure 1), and z is the distance along the member. For m half-waves the stability of the angle of Figure 1 is shown in Figure 2. Consider for example P_{cr} at a length of 3000 mm: the lowest mode is flexural ($m=1$), the 2nd mode is local/torsional ($m=1$), the 3rd and higher modes (up to at least the 8th) are local/torsional modes with more half-waves (m 's) all at about the

same P_{cr} value. This “plateau” of local/torsional P_{cr} values for higher and higher m is usually a characteristic of local buckling and suggests that the local/torsional mode may act *both* like a local mode (with a consistent P_{cr} , i.e., the plateau for higher m values) and a global mode (for long length $m=1$ torsional becomes flexural-torsional and drops off just like all global modes). Further, for thinner (more locally slender) angles this plateau of local P_{cr} values is even more pronounced.

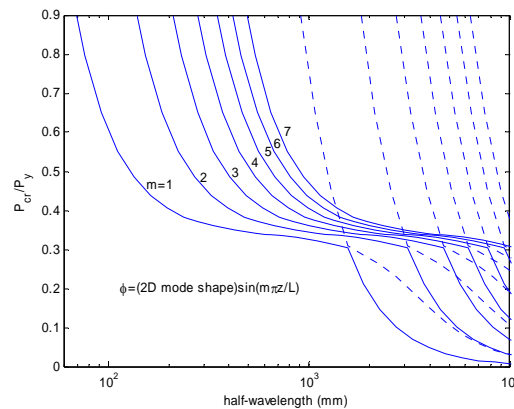


Figure 2 FSM analysis showing m half-wavelengths in any given length

Elastic stability of angles may also be assessed by shell element FE analysis. A particular advantage of the use of shell element FE analysis (e.g., as compared to FSM analysis) is the ease with which more complicated boundary conditions may be treated. For the 60 mm x 60 mm x 2.38 mm angle under study here, a 10 x 10mm mesh of SHELL181 elements was selected in ANSYS, previously shown to provide adequate convergence (Chodraui & Malite 2005). The resulting buckling modes shapes are shown in Figure 1b. For the flexural modes ANSYS and CUFSM are essentially coincident. For the local/torsional mode ANSYS (employing fixed warping conditions at the member ends) gives slightly higher eigenvalues; however, the differences are small because for the studied angles the response is in the plateau region. Further, in CUFSM one can use a $K_t L$ of $0.5L$ to reflect the torsional fixity and again find near coincidence with ANSYS.

3. Sao Paulo Tests

A series of tests on cold-formed steel columns, including angles, were recently performed at the School of Engineering of Sao Carlos – University of Sao Paulo (Chodraui & Malite 2005). The tests, performed on 60 mm x 60 mm x 2.38 mm single and double angles (Figure 3) are briefly summarized here.

Geometric alignment of the member was provided by careful positioning of the endplates and by the presence of guide lines which were made on the bearings, to ensure concentric loading. For single angles, the test's pin-ended bearings allow rotation about the minor axis, while restraining major axis rotations as well as twist rotations and warping. The specimens were positioned so that their minor principal axis coincided with the axis of the support rotation, forcing the specimen to bend about the minor principal axis as illustrated in Figure 4. The effective length (L_r) was taken as $L_{\text{member}} + 135\text{mm}$, due to the distance between the specimens and the pin center for both bearings. For double angles twist and warping was restrained at the ends, but free rotation about the minor and major axis was considered .

Load was applied through a servo-controlled hydraulic actuator in displacement control at a rate of 0.005mm/s. Results from the testing are summarized in Table 1. Material testing taken directly from the specimens indicated $F_y = 37.5 \text{ kN/cm}^2$ and that the actual thickness is 2.38mm (given a nominal thickness of 2.25mm). These values are used for all subsequent analysis.

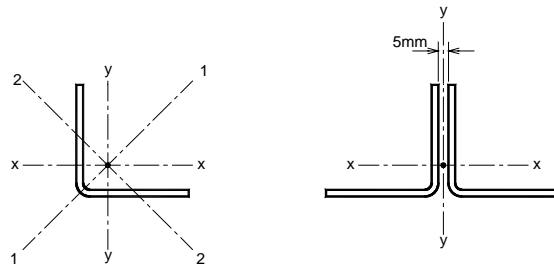


Figure 3 Single and double angle's cross section

Table 1 Tested members and NAS (2004) prediction

SECTION	L_r (mm)	L_{member} (mm)	A (cm^2)	Test P_{test} (kN)	NAS (2004)* P_n (kN)	P_{test} / P_n
L 60x2.38	615	480	2.76	32	26.70	1.20
$K_1 L_r = 0.5L_r$	970	835		28	26.60	1.05
$K_2 L_r = 1.0L_r$	1,330	1,195		24	26.40	0.91
$K_4 L_r = 0.5L_r$	1,685	1,550		24	22.40	1.07
2L 60x2.38	1,045	910	5.53	76	49.80	1.53
$K_x L_r = 1.0L_r$	1,620	1,485		70	49.60	1.41
$K_y L_r = 0.5L_r$	2,190	2,055		62	49.30	1.26
$K_4 L_r = 0.5L_r$	2,765	2,630		46	43.70	1.05
2L 60x2.38	1,490	1,355		73	48.70	1.50
$K_x L_r = 0.5L_r$	2,020	1,885		64	47.40	1.35
$K_y L_r = 1.0L_r$	2,550	2,415		55	45.30	1.21
$K_4 L_r = 0.5L_r$	3,060	2,925		50	42.40	1.18

* See Section 5 for further details and discussion of this calculation



(a) fixture details (pin-ended)

(b) local/torsional in test and model ($L_r=970mm$)

Figure 4 Test setup for Sao Paulo tests

4. Tests of Others

A number of other researchers have performed testing on cold-formed steel angles. These tests are briefly summarized here. For example, recent work by Rasmussen (2005, 2006) has relied primarily on the experiments of Popovic et al. (1999) and Wilhoite et al. (1984), as summarized (for pin-ended tests only) in Table 2, Table 3 and Table 4.

Wilhoite et al. (1984) analyzed high strength press-braked steel both in stub and long columns nominally loaded through the centroid. Popovic et al. (1999) tested cold-rolled and in-line galvanized steel, with fixed and pin-ends. Popovic's pin-ended tests were loaded with a nominal eccentricity of $\pm L/1000$ relative to the centroid, thus mimicking an eccentricity generally assumed in design codes. However, in the comparison with design loads, these columns are treated as loaded through the centroid of the gross section.

Table 2 Geometric and material properties (Rasmussen 2003)

Properties	Wilhoite et al. (1984)	Popovic et al. (1999)
Leg (mm)	69.3	50.8
Thickness (mm)	3.00	2.31 / 3.79 / 4.70
F_y (kN/cm ²)	46.5	39.6
E (kN/cm ²)	20,300	20,300

Table 3 Test results presented by Wilhoite et al. (1984) (Rasmussen 2003)

Specimen	L_r (mm)	L_r / r_y	P_{test} (kN)	P_{test} / P_y
1	823	60.5	72.5	0.388
2	1227	90.2	58.3	0.312
3	1227	90.2	60.1	0.322
4	1227	90.2	65.0	0.348
5	1636	120.2	48.4	0.259
6	1636	120.2	52.1	0.279
7	1636	120.2	59.2	0.317
$P_y = 186\text{kN}$ (squash load)				

Testing on cold-formed steel angles also exists from Prabhu (1982) and Young (2004). Prabhu's tests provided pinned end conditions about both principal axis, and Young's provided fully fixed end conditions. These tests are not detailed further here, as they are not used for comparison with design methods (at this time).

Table 4 Test strengths: Popovic et al. (1999) (pinned tests only)

Test	L_r (mm)	t (mm)	P_{test} (kN)	Failure mode*
1	459	2.31	41.7	FT
2	458		47.2	FT
3	676		35.2	Coupled
4	676		40.1	Coupled-ST
5	862		30.9	Coupled
6	863		47.5	F
7	1,088		25.1	Coupled
8	1,088		32.1	F
9	1,285		17.7	Coupled
10	1,286		24.7	F

FT = flexural-torsional; Coupled = coupled flexural/flexural-torsional;
 F = minor axis flexural; ST = snapped-through.

Overall minor axis flexural imperfections were measured by the researchers. Popovic's tests indicated a magnitude of $L/1305$. The Sao Paulo tests (reported in the previous section) had flexural imperfections ranging from as little as $L/2400$ up to $L/1650$. Prabhu's measured imperfections from $L/2000$ up to $L/500$ and Young provides an average value of $L/2360$ for his tests.

5. Comparisons with Effective Width Design Methods

Rasmussen (2005) provides a comprehensive examination of the use of effective width methods in the determination of the strength of angle columns. His proposed methods (i) ignore torsion in global buckling, and (ii) consider concentrically loaded angles as beam-columns due to the shift from the gross centroid to the effective centroid. Rasmussen also provides an approximate means to handle (ii). His methods may be considered as the most agreed upon interpretation of current cold-formed steel design codes, such as NAS (2004), including recently adopted provisions for unstiffened elements under stress gradients.

One argument commonly made for ignoring global torsional buckling (assumption i above) is that torsional buckling is already accounted for in the local buckling reduction in determining the effective area. Inherent in this argument is that local/torsional buckling follows the post-buckling response characterized by local buckling, as opposed to

global buckling. Further, it is important to note for angles with thick enough legs (fully effective) no reduction for local/torsional buckling would occur regardless of length if torsional buckling is ignored.

Here we examine a simpler effective width approach to concentrically loaded angle columns, where the shift from gross to effective centroid is ignored, and strength is calculated based on (i) the column curve for the appropriate global mode (flexure or torsion) resulting in a stress F_n and (ii) an effective area based on local (torsional) buckling at the long column stress, F_n . This simpler approach is compared to the Sao Paulo tests on single and double angles in Table 1 and Figure 5 and Figure 6 - and represents an alternative interpretation of NAS (2004), or equivalently as noted in the following figures AISI (2001).

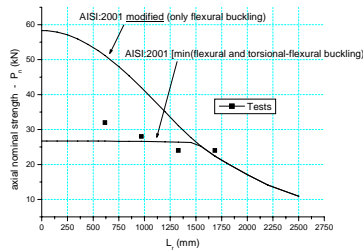
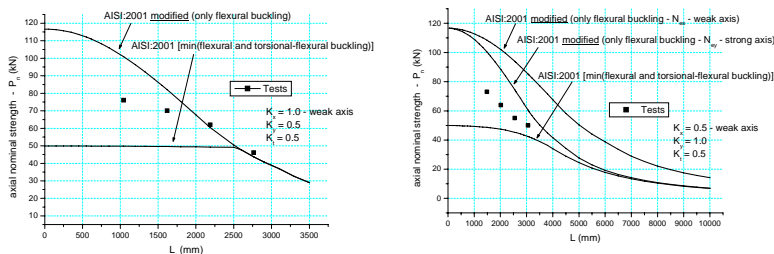


Figure 5 Sao Paulo single angle tests compared with NAS (2004)



(a) weak axis pinned, strong axis fixed (b) weak axis fixed, strong axis pinned

Figure 6 Sao Paulo double angle tests compared with NAS (2004)

Within the context of this design approach the figures suggest that ignoring global torsional buckling in angle columns is unconservative.

The figures are not definitive as this design approach conservatively includes global torsional buckling, but unconservatively ignores shift in centroid. However, as previously discussed in relation to Figure 2, evidence exists that local/torsional buckling may act both as a local buckling mode and a global torsional mode and thus the assumption of ignoring global torsional buckling deserves further scrutiny.

6. Comparisons with Direct Strength Design Methods

The Direct Strength Method (DSM) of design (Appendix 1: NAS 2004, Schafer and Pekoz 1998b) provides a different methodology for calculation of the ultimate strength of cold-formed steel members than the effective width method. For columns, DSM relies on an estimation of the elastic buckling loads (P_{cr}) and the squash load (P_y) to directly provide the strength. The method requires categorization of P_{cr} into one of three types: local, distortional, or global. For angles, questions obviously persist on whether the local/torsional mode should be considered as local, global, or both. Current recommendations (e.g., in AISI 2006) suggest assuming the local/torsional mode can be both local and global. (In fact, it is not inconsistent to assume the mode is distortional – if infinitesimally small lips were added to the angles, the mode would be categorized by most as distortional)

Recently Rasmussen (2006) extended his work on angles to include a DSM approach. Similar to Rasmussen (2005), discussed in the previous section, the work (i) ignores global torsional buckling and (ii) explicitly considers eccentricity – thus requiring a beam-column approach even for nominally concentrically loaded columns. Consistent with DSM the developed beam-column approach uses the stability of the angle under the applied compression + bending stresses which accurately reflects the fact that some eccentricities (away from the legs) benefit the strength and others (towards the legs) do not.

Here, a simplified DSM approach for concentrically loaded angles is explored where the explicit effects of eccentricity are ignored. Six options (a – f) for application of DSM are considered, as detailed in Table 5. The DSM equations are the same as those used in Appendix 1 of NAS (2004) but several choices for P_{cr} are considered.

DSM Options b and c follow the recommendations of Rasmussen and others and ignore L/T as a global mode. Comparison of test-to-predicted ratios in Table 6 indicates that for Wilhoite and Popovic's data this is a reasonable assumption, but for the recent Sao Paulo tests it is quite unconservative. DSM options a, e and f treat local/torsional buckling as both a local-plate mode and global-torsional mode. Options a and e have been recommended for use in the recently completed DSM Design Guide (AISI 2006). Comparisons in Table 6 (of options a, e, and f) show good agreement with the Sao Paulo tests, but conservative solutions for the Wilhoite and Popovic data.

Table 5 Options for application of the Direct Strength Method¹

	a	b	c	d	e	f
P_{cre}	min (L/T,F)	F	F	min (L/T,F)	min (L/T,F)	min (L/T,F)
$P_{cr\ell}$	L/T	L/T	L/T	-	L/T	L/T*
P_{crd}	-	-	L/T	-	L/T	-

¹ Option (e) is conservative and recommended in the DSM Design Guide (AISI 2006)
 $L/T = P_{cr}$ for local/torsional mode (from CUFSM with $K_1L=0.5L$, a more accurate option is to use FE with the exact boundary condition), note: L/T changes as a function of length
 $F = P_{cr}$ for weak primary axis flexural buckling
 $L/T^* = L/T$ but take only at one length, the length where $L/T=F$ (see Figure 1)

Table 6 DSM Options compared with available test data (test-to-predicted ratio)

		a	b	c	d	e	f
Wilhoite	mean	1.27	1.04	1.04	1.14	1.27	1.32
	st.dev.	0.12	0.18	0.17	0.10	0.12	0.14
Popovic	mean	1.18	0.93	0.95	1.06	1.18	1.23
	st.dev.	0.26	0.16	0.16	0.22	0.26	0.28
Sao Paulo	mean	1.00	0.76	0.78	0.91	1.00	1.04
	st.dev.	0.09	0.21	0.19	0.10	0.09	0.10

The lack of agreement between the test methods is somewhat vexing as the actual geometry and material properties tested are quite similar (see summaries in Section 3 and 4). The scatter in the data is shown and compared with a subset of the DSM predictions in Figure 7. Popovic's

data generally follows a reduced flexural buckling, Wilhoite's is hard to discern trends in, and the Sao Paulo tests show the strongest reductions and show little trend against the flexural slenderness. Additional testing and detailed nonlinear finite element analysis would seem to be needed to provide some order to this confusing array of test data.

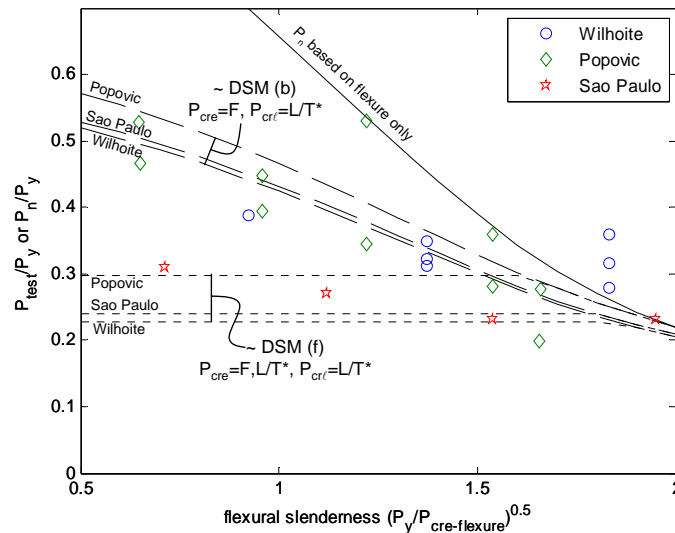


Figure 7 Comparison of test data with strength predictions

7. FE Modeling of Sao Paulo Tests

Nonlinear finite element models of the sections tested in Sao Paulo were developed to better understand the imperfection sensitivity of these sections, and to provide the necessary modeling inputs so that further parametric studies may be conducted in the future. The models were developed in ANSYS. The angles were modeled with 10mm x 10mm shell elements (SHELL181) and the boundary conditions were modeled with a combination of shell elements and continuum elements (SOLID 45). The corners of the angles were modeled explicitly. The boundary conditions represent the tests, with shell and solid elements

respectively used for the member and the bearing (end plates and pinned system) – see Figure 4.

Both local and overall geometric imperfections are found in the columns. Hence, for generating the imperfect member superposition of both modes were considered from the previous eigenbuckling analysis (Figure 1b). The local/torsional imperfection magnitude was determined from type II imperfections in Schafer and Pekoz (1998). Imperfection magnitudes were selected at 25% and 75% probability of exceedance. For the global mode, the imperfection magnitude was found by minimizing the error between measured values and a half sine wave. FEM results are presented in Table 7. Good (slightly conservative) agreement is found between the FE predicted strength and those observed in the test. This provides support that the observed strengths in the Sao Paulo tests are not simply an anomaly.

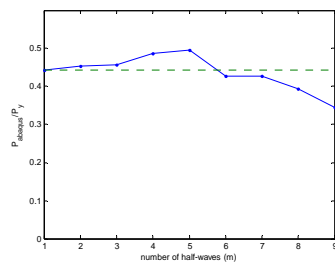
Table 7 Nonlinear FE results versus Tests

Angle 60x2.38mm	P (kN)		
	$K_1.L_r = 0.5.L_r$; $K_2.L_r = 1.0.L_r$; $K_t.L_r = 0.5.L_r$		
L_r (mm)	FEM model 75% / 25%	Test	Test/FEM 75% / 25%
615	30.84 / 26.27	32	1.04 / 1.22
970	27.82 / 24.47	28	1.01 / 1.14
1,330	26.35 / 22.71	24	0.91 / 1.06
1,685	22.50 / 19.85	24	1.07 / 1.21
Average			1.01 / 1.16
st. dev			0.07 / 0.07

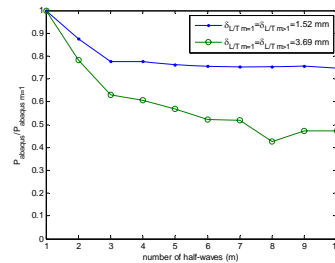
8. Extended FE Modeling of Angles

Additional nonlinear finite element modeling on concentrically loaded cold-formed steel angles was conducted to explore further the potential interactions and imperfection sensitivity between the stability modes. These models were developed in ABAQUS, used pinned free-to-warp boundary conditions, S9R5 shell elements, and included geometric nonlinearity as well as material nonlinearity in the form of von Mises yield criteria with isotropic hardening and a simplified elastic-plastic with strain hardening σ - ϵ curve ($F_y = 345$ MPa).

For a 60 mm x 60 mm x 4.76 mm angle of length 1000 mm Figure 8a demonstrates the predicted imperfection sensitivity of an angle failing in global flexural buckling seeded with imperfections of $L/500$ for the flexural mode and $d/t=0.64$ for a local/torsional mode with m half-waves along the length. Figure 8a demonstrates that local/torsional modes can interact with a global flexural failure, but the interaction is only detrimental when the half-wavelength of the local/torsional mode is short (m large) and thus the local/torsional twist is repeated several times along the length.



(a) Global flexural and local/torsional imperfection with m half-waves



(b) Global torsional ($m=1$) and local/torsional imperfection with $m>1$ half-waves

Figure 8 Strength sensitivity to local/torsional imperfections with m half-waves

A 60 mm x 60 mm x 2.38 mm angle was studied for the possibility of local-plate – global-torsional interaction, i.e., imperfection sensitivity between local/torsional with a single half-wave ($m=1$) and local/torsional with multiple half-waves along the length ($m>1$). The length of the angle was shortened such that the lowest global mode was torsion, not flexure, $L = 615$ mm ($L = 970$ mm was also studied with similar results). The results shown for two imperfection magnitudes are provided in Figure 8b. Even though the higher m local/torsional (L/T) imperfections are orthogonal to the constant L/T $m=1$ imperfection, the predicted strength continues to degrade, showing a definite interaction.

While these limited studies are by no means definitive they do indicate (i) that local/torsional buckling interacts with flexural buckling (as generally understood), and (ii) local/torsional interaction with itself,

albeit at different wavelengths, is possible and detrimental. This supports the notion that local/torsional buckling should be considered as both a local-plate mode and a global-torsional mode in design.

9. Conclusions

Concentrically loaded, equal leg, constant thickness, cold-formed steel angles suffer from two potential instabilities (i) local-plate/global-torsional and (ii) flexural. The coincidence of the local-plate and global-torsional modes complicates the interpretation of elastic stability analysis and design. Through consideration of the possibility of multiple (m) buckling waves along the length of a member it is shown that the local-plate/global-torsional modes may be considered as both a local ($m>1$) and a global ($m=1$) mode. Recently performed tests at Sao Paulo on single and double angles are described and compared with effective width and Direct Strength Methods. The tests indicate that the practice of ignoring local/torsional buckling as a global mode may be unconservative. This contradicts earlier testing, which is also reported in the paper, and thus makes it difficult to come to a definitive conclusion. Further work, supporting the Sao Paulo tests was completed through verification of the tested strengths with nonlinear finite element analysis. In addition a brief parametric study indicated that local/torsional imperfections can have detrimental interactions when the number of half-waves of the imperfections differ (i.e., $m=1$, and $m=8$). Based on these findings it is concluded that the best current practice for design (by effective width or Direct Strength Method) is to treat local/torsional buckling as both a local mode and a torsion mode. It is postulated for long length's the local mode should follow the $m>1$ plateau while the global mode would follow the $m=1$ torsion curve.

Acknowledgments

Research conducted in this paper was supported in part by FAPESP (Sao Paulo State Research Support Foundation – Brazil), USIMINAS (Brazilian Steel Company) and CMS-0448707 of the United States National Science Foundation.

References

- American Iron and Steel Institute (2006). Direct Strength Method Design Guide. American Iron and Steel Institute, Washington, DC. (Approved, to be published in 2006).
- North American Specification (2004). Supplement 2004 to the North American Specification for the Design of Cold-Formed Steel Structural Members: Appendix 1, Design of Cold-Formed Steel Structural Members Using Direct Strength Method. American Iron and Steel Institute, Washington, D.C.
- American Iron and Steel Institute (2001). North American Specification for the Design of Cold-Formed Steel Structural Members. Washington: AISI.
- Chodraui, G.M.B.; Malite, M. (2005). Theoretical and experimental analysis on cold-formed steel members under compression. School of Engineering of Sao Carlos – University of Sao Paulo. Final Report (in Portuguese).
- Popovic, D.; Hancock, G.J. and Rasmussen, K.J.R (1999). Axial Compression Tests of Cold-Formed Angles. *Journal of Structural Engineering*, American Society of Engineers. 125 (5): 515-523.
- Schafer, B.W. (1997). Cold-Formed Steel Behavior and Design: Analytical and Numerical Modeling of Elements and Members with Longitudinal Stiffeners. PhD. Dissertation, Cornell University, Ithaca
- Schafer, B.W. (2001). Finite strip analysis of thin-walled members. In: CUFSM: Cornell University – Finite Strip Method.
- Schafer, B.W.; Peköz, T. (1998). Computational modeling of cold-formed steel: characterizing geometric imperfections and residual stresses. *Journal of Constructional Steel Research*, v.47, 193-210.
- Rasmussen, K.J.R. (2003). Design of Angle Columns with Locally Unstable Legs. Department of Civil Engineering, Research Report No. R830, University of Sydney. Australia.
- Young, B. (2004). Tests and Design of Fixed-Ended Cold-Formed Steel Plain Angle Columns. *J. Struct. Eng.*, 130(12), 1931-1940.
- Yu, W.W. (2000). Cold-Formed Steel Design. New York: John Wiley & Sons. 756p.